

# Assessment of Heat Transfer and Friction Characteristics in Circular Pipe Utilizing Balls as Tabulators

Ali Shokor Golam , Ahmad Muneer El-Deen Faik , Hayder Mohammad Jaffal 

Mechanical Engineering Department, College of Engineering, Mustansiriyah University, Baghdad, Iraq

\*Email: [ali.shokor49@uomustansiriyah.edu.iq](mailto:ali.shokor49@uomustansiriyah.edu.iq)

## Article Info

Received 11/02/2024

Revised 30/11/2024

Accepted 01/12/2024

## Abstract

Flow turbulization is one of the most commonly used techniques for improving heat transfer. This study uses numerical simulation and experimental tests to examine ball turbulators' effect on fluid friction and heat transfer characteristics in a circular pipe. Ball turbulators with different diameters of 10, 15, and 20 mm and spacer lengths of 20 cm are inserted in the circular pipes. The ratio of the diameter of the ball to the diameter of the internal flow path of the pipe, ball turbulent ratio (BTR) =  $D_b/D_p$ , becomes 0.41, 0.62, and 0.83. The water was a working fluid with Reynolds numbers 3,500 to 11,500. The findings demonstrate excellent agreement with deviations of less than 11%. The maximum thermal performance factor reached about 1.18, 1.24, and 1.4 for the BTR 0.41, 0.62, and 0.83, respectively. The ball turbulators increase friction factor; this increase in experimental findings is 52, 65, and 78% at BTR 0.41, 0.62, and 0.83, respectively. Also, it is noticeable that there is a gradual decrease in thermal performance when the Reynolds number range is higher than 7500.

**Keywords:** Ball turbulators; Enhancement of Heat Transfer; Thermal performance factor; Thermo-Hydraulic Characteristics

## 1. Introduction

Improving heat exchangers' thermal and hydraulic performance is an important priority in all industrial systems that use heat exchangers. Reducing the size of the heat exchanger, increasing heat transfer efficiency, and saving energy are among the most important problems previously studied. Studying the thermal behavior in a single channel enables us to evaluate the performance of the heat exchanger [1]. Many extensive experimental and numerical studies were reviewed to clarify the factors and mechanisms studied within our current field of study. Charun [2] examined the geometrically a ball tubulising insert in a vertical pipe. Four distinct insert types were studied with one variable parameter: various ball diameters in the  $Re = 3000 - 30,000$  range. There was no longitudinal distance between the balls to be studied as a second criterion in that research since the balls were always next to one another, forming a cascade. For the largest ball diameter, the highest Nu values, as well as the highest flow resistance, were determined. The smallest-diameter balls produced a slight pressure decrease and slightly enhanced heat transmission. A numerical investigation used a commercial computational fluid dynamic (CFD) code to study helical tabulators with various pitches. Sahin [3] stated that the proposed tabulators may increase heat

transfer quantity by around 2-3 times compared to smooth pipes. To examine the heat transfer, pressure loss, and thermal performance of a BT insert in a circular pipe operating at a high Reynolds number of (10,000 -300,000) [4]. Jasi'nski [5]-[7] employed computational methods. According to the results, the heat transfer rate may be significantly boosted by employing bigger balls and placing them closer together. However, the pressure drop increases more as the heat augments. Using triple-start corrugated pipes, Promthaisong et al. [8] investigated the effects of various design factors on heat transfer and turbulent flow behaviors. According to their research, adopting a corrugated type triple-start may increase helical swirl flow and swirl flow, which reduces the thickness of the thermal boundary layer and speeds up heat transfer in pipes. Man et al. [9] studied the impact of different-sized twisted tapes on heat transfer enhancement via a circular conduit. According to the results, the geometrical characteristics of the twisted tape seemed to have a considerable impact on improving thermal performance. Yuan et al. [10] studied the effect of ball bearings (Bts) on fluid heat transfer and frictional properties in a circular pipe through numerical simulation. A single circular tube was used to study the effect of inserting metal balls with different diameters (0.5, 0.75, and 1) mm fixed on a thin rod with distances (40, 51.77, and 62.5) mm between them. It was found that the improvement

rate in heat transfer reaches 1.26 and 2.01 when compared with the smooth tube. It was also found that using larger diameter balls and smaller distances increases the heat transfer rate but leads to flow pressure loss. Zhang et al. [11] studied the effect of the width of the spiral stripes (7.5, 12, 15, and 20 mm) on the performance of the heat exchanger. The results showed that the 15 mm wide spiral strip gave the highest thermal performance. Murthy et al. [12] conducted a study on the effect of combining passive techniques on the performance of a double-tube heat exchanger. Twisted ribbons of varying composition (twist ratio: 20, 13.3, and 9.8) and helical ribbons were combined using Al<sub>2</sub>O<sub>3</sub> Nanofluid in different proportions. The results showed that the Nusselt number increases by 11% and the thermal performance increases by 1.116 times in the case of using twisted ribbons with a twist ratio of 20 and 0.05% Nano fluid mixture, and by 24.93% and 1.269 times in the case of repeatedly spaced helical spiral ribbons. Veera et al. [13] analyzed the energy behavior of an evacuated tube with a solar air collector (ETIBSAC) with different loose perforated twisted tape (LFPTT) design configurations. The highest thermal efficiency was 62.33% at  $(y/D) = 2$  and 400 kg/h when ETIBSAC was used with LFPTT. On the other hand, the highest efficiency was found to be 3.91% at  $(d/D) = 0.0714$ . Hosseinejad et al. [14] studied the effect of inserting a twisted ribbon inside a smooth tube. Their results showed that the Nusselt number increases with increasing Reynolds number and twist ratio of the twisted ribbon, thus improving the heat transfer process. Labib et al. [15] conducted experimental and numerical analyses to study the effect of twisted tape inclusions on the flow behavior and heat transfer in double-tube heat exchangers. A twisted bar with different twist ratios (7.5, 6, and 4.5) was used. In both studies, the Reynolds number ranges from 15,000 to 50,000. The results show good agreement between the numerical and experimental results and that the numerical model predicts reliably for studying flow behavior and heat transfer in heat exchangers. Also, it has been shown that the use of twisted tapes enhances the thermal performance of the exchangers at all twisting ratios mentioned. In an experimental study, Bhuiya et al. [16] compared tabulators with tiny v-cut inserts on the edges versus tabulators without concentrating on how water flows through pipes. The findings demonstrated that when the pitch ratio decreases, the average Nu number and friction factor rise in both pipes, irrespective of the tabulator. Luo et al. [17] studied the heat transfer efficiency in heat exchangers using a DNA-like twisted strand. The effect of section pitch (1 to 4) mm was analyzed to evaluate its effect on heat transfer properties. The results indicate that using the aforementioned twisted tape with a step ratio of 2 mm increases the heat transfer efficiency by up to 125% compared to a regular tube. It was also shown that combining the twisted tape with a spiral wire wrapped around it increases heat efficiency by up to 142%. Eiamsa-ard et al. [18] presented an experimental study to investigate using a delta-wing twisted bar to improve heat exchanger efficiency. Compare the effect of using straight (S-DWT) and oblique (O-DWT) delta wing twisted tape. The analysis of the experimental results found that using the oblique delta wing twisted tape (O-DWT) is more effective in transferring heat than the other type. Srivastava et al. [19] used cones as turbulent bodies for the flow path of a heat exchanger tube. They also studied the effect of inserting perforated and

non-perforated conical pieces. The results showed that using conical pieces succeeded in mixing the fluids flowing in the core of the tube and adjacent to the inner walls. At a Reynolds number of 6258, it was found that the inserts of the perforated cones achieved a maximum heat transfer capacity of 1.38 times compared to a plain tube. Nakhchi et al. [20] conducted a numerical study, finding that louvered strips with holes allow more heat to pass through than solid ones. The research found that the perforations in the louvered strips disrupted the recirculation flow, which increased the dissipation of turbulent kinetic energy. The thermal performance of a corrugated pipe with the wire coil as a swirl generator was studied statistically by Kazemi et al. [21]. This research looked at how changing certain of the wire coil's geometric factors affected the improvement in heat transmission. The results showed that the heat transfer rate was significantly improved using the corrugated pipe and the wire coil. The literature reviewed for previous studies investigated methods for improving heat exchangers' hydraulic and thermal performance. Previous studies indicate that complex factors, mechanisms, and effects are involved in the phenomenon of heat transfer when turbulence is inserted into the flow path. The majority of studies were related to the spring's insert, twisted, and wavy insertion tapes placed inside the flow path. Recently, researchers have been interested in using balls to improve the performance of heat exchangers, such as [5]-[7], [10]. Due to the lack of investigations related to inserting turbulent parts, such as those carried out in this study, there is a need to further delve into and analyze the technique of using balls as turbulent bodies for flow inside pipes. To achieve this goal, in this work, light and focus were highlighted on studying the ratio of the diameter of the ball to the diameter of the internal flow path of the pipe, ball turbulent ratio (BTR) =  $D_b/D_p$ , while fixing the distance between the balls. By analyzing the experimental results and numerical simulation of a smooth pipe before and after introducing spherical turbulence, we explored the flow properties represented by heat transfer and pressure losses.

## 2. Numerical Simulation

### 2.1. Physics Model

The water enters the pipe at a temperature of 298 k. The surface of the pipe is exposed to a constant heat flux, so the water gains heat. Balls of different diameters were inserted to increase turbulence inside the pipe and improve heat transfer. The smooth pipe will be used as a basis for evaluating the exchanger's performance with the balls used. Fig.1 depicts the physical representation of a circular pipe with Bts inserted.  $L = 1000$  mm and  $D = 24$  mm, respectively, are the copper pipe's overall length and inner diameter.

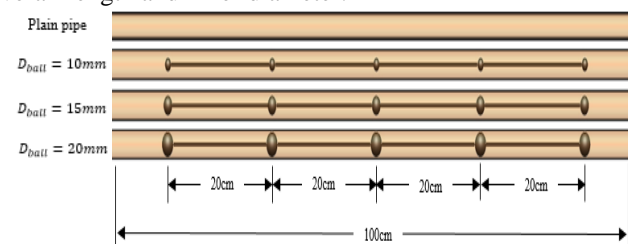


Figure 1. Bts-inserted circular pipe model.

## 2.2. Governing Equations and Boundary Conditions

For numerical model simplification, the following assumptions are made to solve the governing equations:

- The water's physical characteristics remain constant.
- The flow is steady, incompressible, and turbulent.
- Thermal radiation, natural convection, and gravity have been ignored.
- The thin rod on which the balls are mounted and holds them in an axial position is neglected.
- No slip conditions are placed on the Bts surfaces or the pipe walls.
- The location of the balls in the center of the pipe.

The location of the balls was imposed in the center of the pipe because most of the time, in the state of their movement with the flow, they are in the center, as the natural movement is random, hitting the wall and then moving to the center of the pipe. Therefore, this assumption was made to facilitate the solution. The flow will be the same result in heat transfer and pressure drop because when the ball moves away from one side, it approaches the other side, meaning that the heat transfer remains constant on one side and increases on the other. The same case is for the pressure drop, so it is reasonable to assume that the ball is in the center of the pipe.

The following tensor form equations for continuity, momentum, and energy are provided [22]:

### Continuity equation:

$$\frac{\partial \rho}{\partial t} + \frac{\partial(\rho u_i)}{\partial x_i} = 0 \quad (1)$$

### Momentum equation:

$$\frac{\partial(\rho u_i)}{\partial t} + \frac{\partial(\rho u_i u_j)}{\partial x_j} = -\frac{\partial p}{\partial x_i} + \frac{\partial}{\partial x_j} \left\{ \mu \left( \frac{\partial(u_i)}{\partial x_j} + \frac{\partial(u_j)}{\partial x_i} \right) - \rho u_i^- u_j^- \right\} \quad (2)$$

$$-\rho u_i^- u_j^- = \mu_t \left( \frac{\partial(u_i)}{\partial x_j} + \frac{\partial(u_j)}{\partial x_i} \right) - \frac{2}{3} k \delta_{ij} \quad (3)$$

### Energy equation:

$$\frac{\partial}{\partial t}(\rho E) + \frac{\partial}{\partial x_i} [\mu_i(\rho E + p)] = \frac{\partial}{\partial x_i} \left[ k_{eff} \frac{\partial T}{\partial x_i} \right] \quad (4)$$

The RNG k-ε turbulence model was chosen for the computational solutions. The k-ε equations associated with the turbulence model are as follows [23]:

$$\begin{aligned} & \frac{\partial}{\partial t}(\rho k) + \frac{\partial}{\partial x_i}(\rho k v_i) \\ &= \frac{\partial}{\partial x_j} \left[ \left( \frac{\mu + \mu_t}{\sigma_k} \right) \frac{\partial k}{\partial x_j} \right] + \mu_t \left( \frac{\partial v_i}{\partial x_j} + \frac{\partial v_j}{\partial x_i} \right) \frac{\partial v_i}{\partial x_j} \\ & - \rho \varepsilon \end{aligned} \quad (5)$$

$$\begin{aligned} & \frac{\partial}{\partial t}(\rho k) + \frac{\partial}{\partial x_i}(\rho k v_i) \\ &= \frac{\partial}{\partial x_j} \left[ \left( \frac{\mu + \mu_t}{\sigma_\varepsilon} \right) \frac{\partial \varepsilon}{\partial x_j} \right] + C_{1\varepsilon} \frac{\varepsilon}{k} \mu_t \left( \frac{\partial v_i}{\partial x_j} + \frac{\partial v_j}{\partial x_i} \right) \frac{\partial v_i}{\partial x_j} - C_{2\varepsilon} \rho \frac{\varepsilon^2}{k} \\ & - \alpha \rho \frac{\varepsilon^2}{k} \end{aligned} \quad (6)$$

$$\mu_t = \rho C_\mu \frac{k^2}{\varepsilon} \quad (7)$$

Here, the thermal-hydraulic computation uses the shear stress transfer (SST) k-turbulence model, especially when there is a stream separation. The SST model's key characteristic is its capacity to account for a viscous sublayer by using the k-model close to the wall and the conventional k-model in the turbulent core. The tested inserts had this flow pattern. Reference [24] includes a thorough examination of this model by Menter. The velocity-inlet boundary condition is established, and the constant heat flux condition is stated on the pipe wall. The temperature of the flowing water is 298 K, and the flow velocity ranges from (0.12 to 0.42) m/s with a constant increase rate of 0.075 m/s. A Reynolds number is generated from (3500 to 11500) based on the flow velocity. The Reynolds number was chosen within the mentioned rate to ensure the water flows within a turbulent flow pattern. The pressure-outlet boundary condition is further used.

The meshes were created using ANSYS Fluent 19 R3 software, as shown in Fig.2. The hexagonal grid was used to generate the mesh. The boundary layers were subjected to the local grid refinement rule, and this mesh model additionally included adaptive grid refinement. Four grid conditions were used to perform the grid selection tests. As shown in Table 1, the test was performed at a heat flux of 2000 W/m<sup>2</sup> and a Reynolds number of 7500 under the influence of spherical turbulences BTR of 0.41, 0.62, and 0.83. The results found that the grid systems 1,609,342, 1,601,647, and 1,621,786 are dense enough to be considered in the numerical simulation. The numerical simulation used the computational fluid dynamics (CFD) software. The finite-volume approach assessed the above equations with the given boundary conditions. The second-order upwind technique was used in the equations to simulate the momentum, turbulent kinetic energy, and turbulent dissipation rate. The semi-implicit SIMPLE method was used in the numerical solution process.

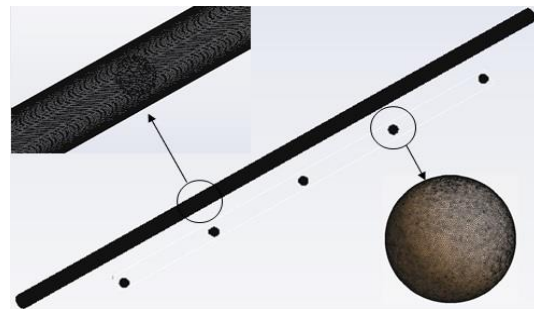


Figure 2. Mesh was created for pipe and balls.

Table 1. Grid independency test at Re = 7500, Q = 2000 W/m<sup>2</sup>.

| BTR   | Size of Grid | Nu     | f      |
|-------|--------------|--------|--------|
| 0.41% | 948,376      | 64.714 | 0.0619 |
|       | 1,245,656    | 67.854 | 0.0749 |
|       | 1,609,342    | 68.745 | 0.0771 |
| 0.62% | 2,189,901    | 68.821 | 0.0782 |
|       | 973,102      | 70.981 | 0.0963 |
|       | 1,189,458    | 71.351 | 0.109  |
|       | 1,601,647    | 71.699 | 0.112  |

|       |           |        |       |
|-------|-----------|--------|-------|
|       | 2.105,937 | 71.811 | 0.115 |
|       | 981,828   | 78.906 | 0.139 |
| 0.83% | 1,205.598 | 79.291 | 0.164 |
|       | 1,621,786 | 79.884 | 0.167 |
|       | 2,163.783 | 80.029 | 0.17  |

### 3. Experimental Work

The present section briefly describes the experimental test platform and the turbulence model (balls) used in our present work. Fig. 3 shows the test apparatus. The test platform parts were carefully manufactured and assembled to prevent water leakage during the tests. A 200-liter water tank made of stainless steel supplies cold water via a pump to the heat exchanger. The tank is 60 cm in diameter and 90 cm in height. The heat exchanger is a smooth copper tube well insulated to prevent heat dissipation. The other most important part of constructing the tester is the centrifugal water pump, which operates at a constant voltage of 220V and 2.5A, with  $Q_{max} = 30$  L/m and  $H_{-Max} = 30$ m. The test device is also outfitted with a Variac 3000W for power control. In most cases, testing only one pipe (channel) is sufficient to evaluate the efficiency of the complete heat exchanger since the heat transfer in one channel of the heat exchanger represents the overall efficiency of the entire device. Five K-type thermocouples were used to measure the temperature. Two monitored the water temperature at the inlet and outlet of the heat exchanger, and three were distributed along the heat exchanger with a distance of 250 mm between them. To monitor temperatures and record those readings permanently, all thermocouples are linked to the HT-9815 four-channel data logger. A single flow meter (type-LZS) was used, and 12 mm diameter polyvinyl chloride (PVC) tubing was used to connect all tester parts due to its flexibility and ease of reinstallation after maintenance. More details about the measuring devices are shown in Table 2.

**Table 2.** Details of the measuring devices.

| Devices       | Description | Range            | accuracy                         |
|---------------|-------------|------------------|----------------------------------|
| Thermo-couple | Type- K     | -100 to 1300°C   | $\pm 1.1^\circ\text{C}$ or 0.4%. |
| Data recorder | HT-9815     | -200 to 1372 °C  | $\pm 1^\circ\text{C}$ or 0.3%.   |
| Flow meter    | Type-LZS    | 100 to 1500(L/H) | $\pm 4\%$                        |

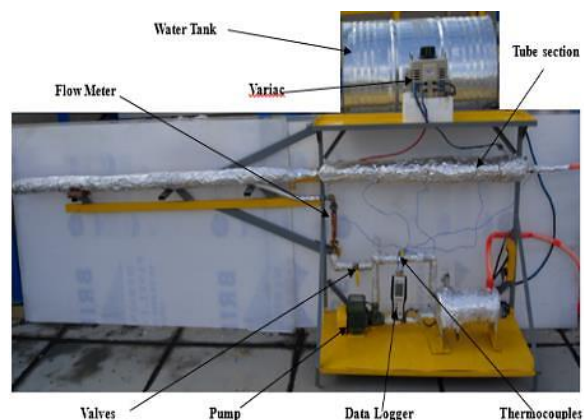


**Figure 3.** Experimental test rig.

A 3000 W electric heater consisting of a 1.5 mm diameter wire and 3 m long was used to wrap around the test tube. The test tube is a smooth copper tube with a length of 1 m and an internal diameter of 24 mm. An electrical insulator is used to wrap around the entire test tube to help isolate the tube from electrical contact and distribute the applied heat flux along the tube evenly, as shown in Fig. 4. While the water inlet temperature and operating conditions were stable in all experiments, the thermal and hydraulic performance of the smooth tube was studied before and after introducing BTS turbulence models by varying the water flow rates and the applied heat flux on the tube surface.

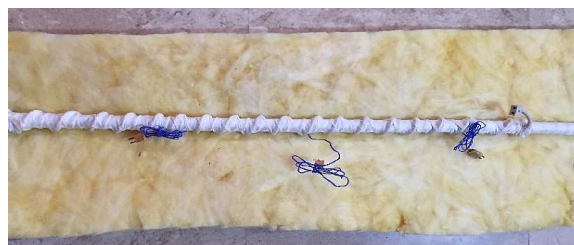


**Figure 4.** Test Section.

Details of the metal ball, made of Iron steel alloy, and its distribution inside the pipe are shown in Fig 5. Ball actuators with different diameters of 10, 15, and 20 mm and spacer lengths of 20 cm are inserted into the circular tubes. The thin rod was fixed in the center of the balls, and oxyacetylene torch welding was used to attach the rod to the balls. Three different diameters of the metal balls, 10, 15, and 20 mm, were used to make the BTR 0.41, 0.62, and 0.83, respectively. The balls were distributed inside the tube and installed in the center of the tube in a way that prevented them from coming into contact with the inner walls of the copper pipe (to ensure the prevention of heat transfer from the surface of the inner pipe to the body of the balls). Their function was only to act as turbulent bodies for the flow.



Figure 5. Ball turbulators models and arrangement.

### Data reduction

The amount of electrical energy applied to the surface of the tube can be calculated using the formula [25]:

$$Q_{heater} = I \cdot V \quad (8)$$

Calculating (Nu) the local Nusselt number using the moving ball inside the pipe, where  $Nu_p$  is the local Nusselt number at a smooth pipe [26].

$$Nu = \frac{q'' * 2R}{k_w * (T_w - T_m)} \quad (9)$$

$$q'' = h(T_w - T_m) \quad (10)$$

$$T_m = \frac{T_i + T_o}{2} \quad (11)$$

$$Nu_p = \frac{q'' * 2R}{k_w * (T_{WP} - T_m)} \quad (12)$$

It is difficult to improve thermal performance directly because the increase in fluid flow turbulence causes a significant loss of energy and an increase in the frictional pressure drop in the pipe, which will consume additional energy for pumping. Hence, the design process must be evaluated to obtain the optimal design. The thermal performance factor is calculated using the following equation [27]. The friction factor was obtained at the smooth pipe and when the ball was inserted.

$$f = \frac{2 D_p}{\rho u^2} \left( \frac{dp}{dx} \right)_{pipe \text{ with ball}} \quad (13)$$

$$f_p = \frac{2 D_p}{\rho u^2} \left( \frac{dp}{dx} \right)_{smooth \text{ pipe}} \quad (14)$$

The increase in heat transfer rates through the pipes when using flow turbulence is not considered an improvement unless compared to the friction coefficient, which causes losses in flow pressure. The thermal performance factor (TPF) criterion is the basis for determining the extent of improvement in the heat transfer process of heat exchangers [28].

$$TPF = \frac{Nu/Nu_p}{(f/f_p)^{1/3}} \quad (15)$$

## 4. Results and Discussion

It believes that these results will provide more useful evidence to assist in thermal design in this field and choose the best ratio of the diameter of the ball used relative to the diameter of the pipe's flow path. This section reviews the rapprochement and discussion results of inserting Bts within plain pipe in different ball turbulent ratios (BTR) to improve heat transfer.

### 4.1. Experimental and Numerical Models Rapprochement

To validate the CFD simulation model. Comparisons are made between experimental and numerical results. Comparisons are made using the mean relative error (MRE) defined in Eq. (16).

$$MRE = \frac{1}{N} \sum_{i=0}^N \left| 100 \times \frac{P_i - E_i}{E_i} \right| \quad (16)$$

To validate the numerical procedure described above, Fig.6 and Fig.7 compare the numerical results of the Nusselt number and friction factor with the experimental results for ordinary pipelines at a heat flux of 2000 W/m<sup>2</sup>. The CFD results are in excellent accord, as the Nusselt number and friction factor deviate by less than 6% and 11%, respectively. The difference between experimental and numerical values is due to Uncertainty in the measuring instruments and assumptions made for the numerical simulation.

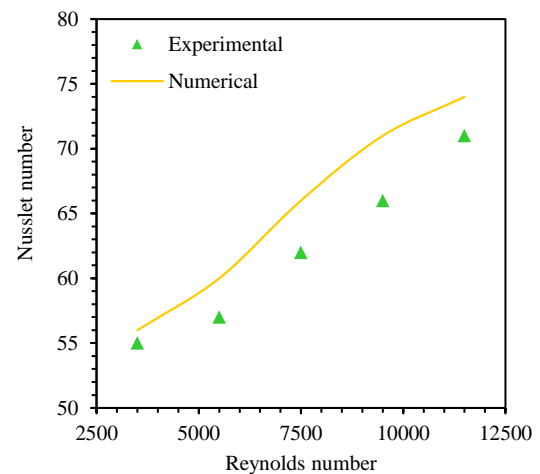


Figure 6. (Nusselt - Reynolds) number data rapprochement for the plain pipe.

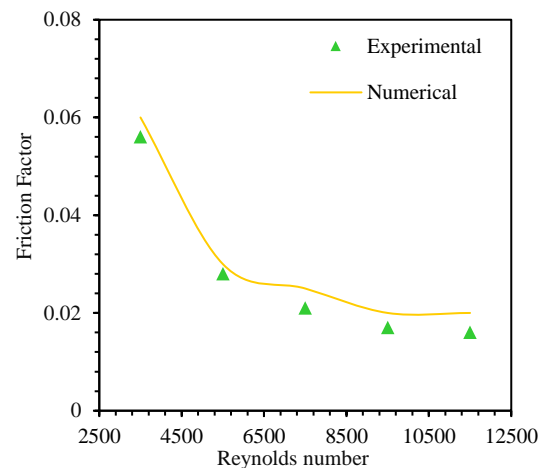
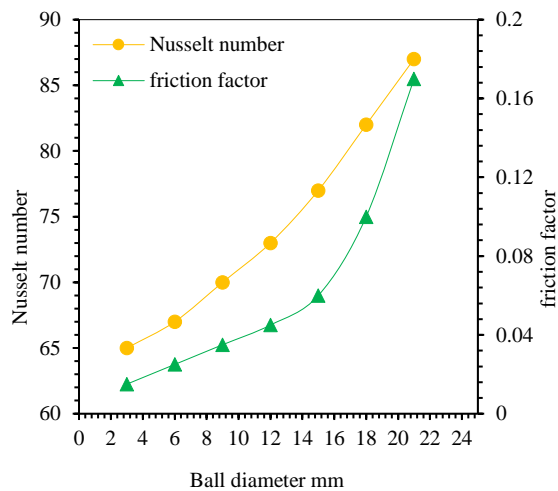


Figure 7. (Friction factor - Reynolds number) data rapprochement for the plain pipe.

## 4.2 Numerical result

### 4.2.1 Influence of Ball Diameter

Since the size of the balls is a significant variable for this study, a wide range of ball diameters was studied in the ANSYS program to reduce the effort, time, and cost of the study on the experimental side, as shown in Fig.8. The diameter of the balls ranged from 3 to 21 mm. The figure shows that an increase in the diameter of the ball leads to an increase in the Nusselt number and the friction coefficient at constant boundary conditions. However, exceeding the diameter of the ball by 15 mm leads to a sudden increase in the friction coefficient due to the occurrence of a throttling flow that is accompanied by an increase in the Nusselt value.

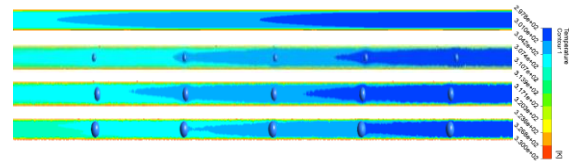


**Figure 8.** Numerical results of ball diameter concerning Nusselt number and friction factor.

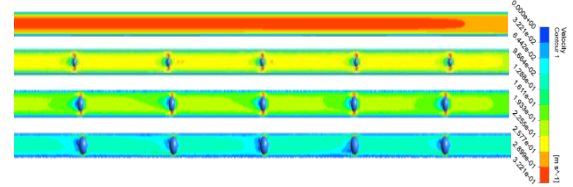
### 4.2.2 Temperature, velocity, and pressure distribution contours

Fig.9 to Fig.11 illustrate temperature, velocity, and pressure distribution contours inside the pipe with and without turbulent balls at heat flux  $2000 \text{ W/m}^2$  and  $\text{Re } 7500$ . Fig. 9 depicts the temperature distribution contours throughout the length of the pipe. It also clearly demonstrates that the temperature of the surface of the pipe near the ball is lower when there is no ball. In addition, the balls model and distribution inside the pipe maintained a temperature gradient near the inner pipe walls and thus enhanced heat transfer from the surface of the pipe to the water. On the other hand, it can be discerned that as the diameter of the balls increases, so does the intensity of turbulence, and hence the amount of heat transferred increases.

Moreover, from the velocity distribution contours in Fig. 10, it can be noted that the velocity of the fluid at the region between the balls and the pipe increases whenever the diameter of the balls increases. In other words, the velocity of the fluid at both sides of the ball increased, making the area near the pipe's inner wall more turbulent, which leads to a reduction in the stagnation area caused by shear stress. As found in Fig. 11, the pressure drop in the pipe rises with the increase in the diameter of the turbulent balls, and the case requires additional pumping force to compensate for the increased pressure drop.



**Figure 9.** Temperature contour inside the pipe with and without turbulent balls.



**Figure 10.** Velocity contour inside the pipe with and without turbulent balls.

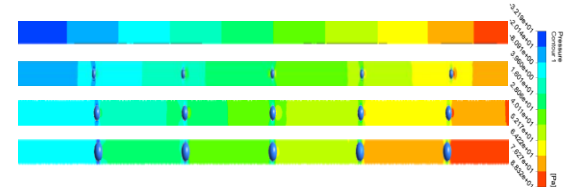


**Figure 11.** Pressure contour inside the pipe with and without turbulent balls.

## 4.3 Experimental result

Fig.12 to Fig.15 illustrates the relationship between the Nusselt number and Reynolds number with and without Bts. In general, the value of the Nusselt number increases with the increase of the Reynolds number and the heat flux applied to the surface of the outer pipe. Most previous researchers have achieved general behavior [5]-[7],[10]. At the same Reynolds number and heat flux applied to the tube surface, BTS patterns were found to significantly affect the Nusselt number when compared to a normal tube. This is because the distribution of BTS patterns inside the tube retards the flow, which promotes the contact of water with the inner tube walls. From the figures, the use of the Bts 20mm ( $\text{BTR} = 0.83$ ) gave the best Nusselt number compared to the rest of the used ball models. The obstructive flow of water enhances the contact with the pipe's inner walls, where we find that the surface temperature of the pipe is reduced when obstructing flow performance is good. The balls prevent the growth of the adjacent thermal boundary layer, considered an insulating layer that prevents heat transfer. On the other hand, the location of the balls can cause more mixing in the flow and generate more vortices, which leads to the destruction of the thermal boundary layer.

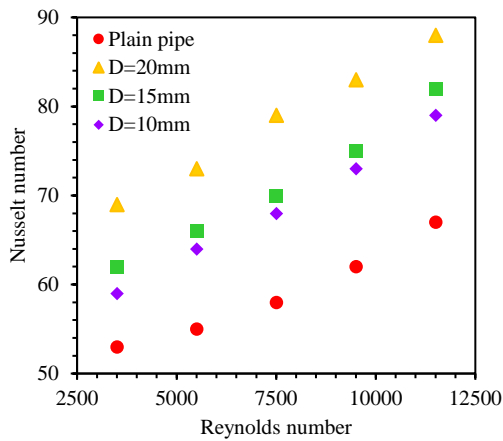


**Figure 12.** Nusselt-Reynolds relationship. (Q = 1500 W/m²)

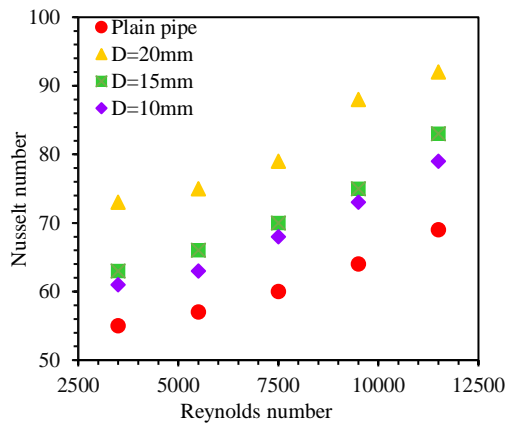


**Figure 13.** Nusselt-Reynolds relationship. (Q = 2000 W/m²)

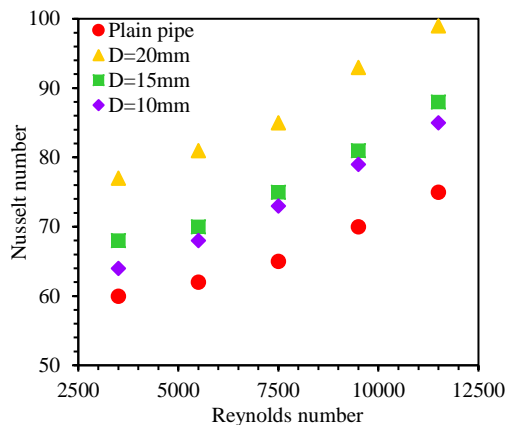


**Figure 14.** Nusselt-Reynolds relationship. (Q = 2500 W/m²)

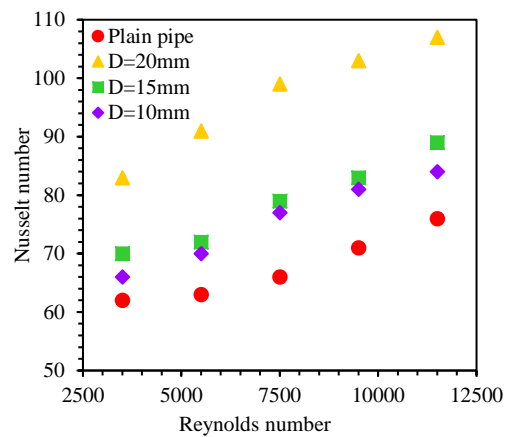


**Figure 15.** Nusselt-Reynolds relationship. (Q = 3000 W/m²).

Unlike the Nusselt number, the friction factor decreases with increasing Reynolds number for all Bts. Fig.16 experimentally illustrates the influence of flow velocity on the friction factor with and without Bts. This figure indicates that the higher the flow rate, the more significant the pressure drop; thus, the friction factor decreases while the friction factor increases with Bts. The Bts inside the pipe increases the friction factor compared to a smooth pipe. This amount of increase in the experimental results is 52% for a ball with a diameter of 10 mm (BTR = 0.41), 65% for a ball with a diameter of 15 mm (BTR = 0.62), and 78% for a ball with a diameter of 20 mm (BTR = 0.83). In other words, the increased flow resistance is because the larger ball diameter ratio leads to increased shear force and decreased pressure. This behavior is consistent with the findings of the researcher [10].

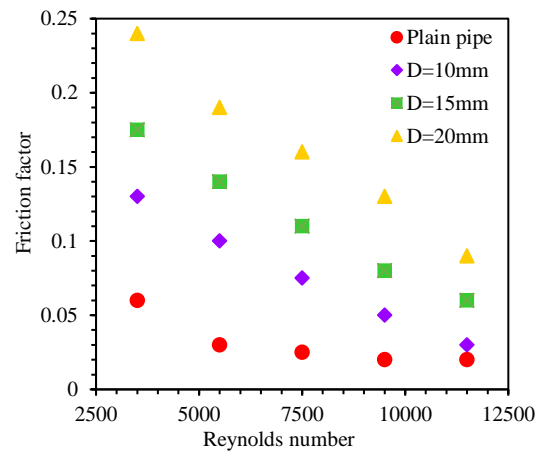


**Figure 16.** Friction factor versus Reynolds number at different ball diameters.

The Nusselt number and the friction factor influence the thermal performance factor. An improvement in thermal performance is defined as an increase in the quantity of heat transmitted that is larger than the increase in the amount of pressure drops. Fig.17 shows the thermal performance factor versus the Reynolds number at different ball diameters. From the figure, the maximum thermal performance factor reached about 1.18 for a 10 mm ball diameter (BTR = 0.41), 1.24 for a 15 mm ball diameter (BTR = 0.62), and 1.4 for a 20 mm ball

diameter (BTR = 0.83). This is because the use of turbulent bodies for flow BTS is more effective in disturbing the boundary layer repeatedly, which creates a disturbance in the water flow. Also, It is noticeable that there is a gradual decrease in thermal performance when the Reynolds number range is higher than 7500, and the explanation for this case is the occurrence of choked flow phenomenon, which occurs at high velocity.

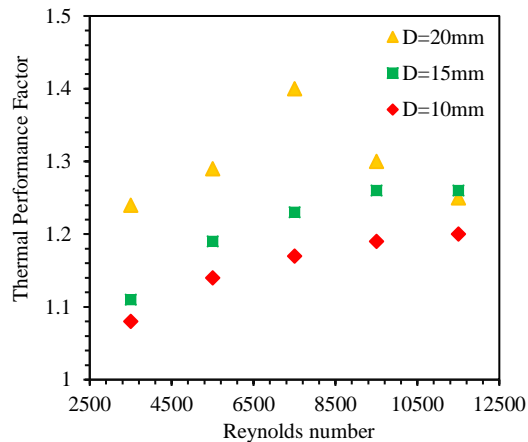


**Figure 17.** Reynolds number and thermal performance factor at various ball diameters.

## 5. Conclusions

The heat transfer characteristics and friction factor of turbulent water flow in a circular pipe equipped with ball turbulators were studied numerically and experimentally. The properties mentioned above were investigated for the effect of using three different diameters of balls 10, 15, and 20 mm, making the ratio of the diameter of the ball to the diameter of the internal flow path of the pipe BTR 0.41, 0.62, and 0.83, respectively. It was observed that there is a good agreement between the numerical and experimental results, with an error ratio that does not exceed 11%. Various conclusions can be observed from this study. In general, as the Reynolds number and heat flux applied to the surface of the outer pipe grows, so does the Nusselt number's value increase. The studied ball turbulator models (Bts) significantly impact the Nusselt number. An increase in the ball's diameter causes an increase in the Nusselt number and friction coefficient. But when the ratio of the diameter of the ball to the diameter of the internal flow path of the pipe BTR = 0.62 is exceeded, the friction coefficient suddenly rises. The ratio of the diameter of the ball to the diameter of the internal flow path of the pipe BTR = 0.83 gave the best Nusselt number compared to the rest of the used ball models. The ball turbulators within the pipe increase friction factor compared to the smooth pipe; this increase in experimental findings is 52% at a BTR = 0.41, 65% at a BTR = 0.62, and 78% at a BTR = 0.83. The maximum thermal performance factor reached about 1.18, 1.24, and 1.4 for the BTR 0.41, 0.62, and 0.83, respectively. Also, It is noticeable that there is a gradual decrease in thermal performance when the Reynolds number range is higher than 7500.

## Acknowledgments

The authors express their gratitude for the assistance provided by the Mechanical Engineering Department at Mustansiriyah University, Baghdad, Iraq, in completing this research project.

## List of Symbols

|                 |                                     |
|-----------------|-------------------------------------|
| Re              | Reynolds number                     |
| p               | Pressure (Pa)                       |
| Nu              | Nusselt number                      |
| $\mu$           | Dynamic viscosity (Pa.s)            |
| t               | Time                                |
| $T_m$           | Mean temperature K                  |
| v               | Velocity                            |
| $T_w$           | Pipe wall temperature K             |
| $\rho$          | Density                             |
| R               | Radius of the pipe m                |
| i, j            | Velocity directions in X and Y      |
| $D_p$           | Pipe diameter m                     |
| $q''$           | Heat flux $W/m^2$                   |
| h               | Heat transfer coefficient $W/m^2.K$ |
| f               | Friction factor                     |
| u               | Velocity of the fluid m/s           |
| $\frac{dp}{dx}$ | Pressure gradient Pa/m              |
| $k_w$           | Thermal conductivity W/m.K          |
| I               | Electric current A                  |
| V               | Electric voltage V                  |
| $T_i$           | Water inlet temperatures K          |
| $T_o$           | Water exit temperatures K           |
| $P_i$           | Maximum value                       |
| $E_i$           | Minimum value                       |

## Conflict of interest

The authors confirm that the publication of this article causes no conflict of interest.

## Authors' contributions:

Ali Shokor Golam (Corresponding author) devised the research methodology, conducted experimental and numerical analyses, drafted the original manuscript, and secured funding for the project.

Ahmad Muneer El-Deen Faik performed formal analysis and investigation and contributed to the original manuscript.

Hayder Mohammad Jaffal: conducted formal analysis and investigation, participated in manuscript writing, reviewed existing literature, and contributed to editing and project administration.

## References

- [1] S. Hasan and Z. H. Naji, "Augmentation Heat Transfer In A Circular Tube Using Twisted - Tape Inserts: A Review," *Journal of Engineering and Sustainable Development*, vol. 27, no. 4, pp. 511–526, Jul. 2023, doi: <https://doi.org/10.31272/jeasd.27.4.8>.
- [2] H. Charun, "Heat Transfer and Pressure Drop in a Vertical Tube with a Nodular Turbulizer," *Applied Thermal Engineering*, vol. 28, no. 14–15, pp. 1984–1994, Oct. 2008, doi: <https://doi.org/10.1016/j.applthermaleng.2007.12.012>.
- [3] H. M. Şahin, E. Baysal, and A. R. Dal, "Experimental and Numerical Investigation of Thermal Characteristics of a Novel Concentric Type Tube Heat Exchanger with Turbulators," *International Journal of*

- Energy Research*, vol. 37, no. 9, pp. 1088–1102, May 2012, doi: <https://doi.org/10.1002/er.2919>.
- [4] I. A. Ghani, N. A. C. Sidik, N. Kamaruzzaman, W. J. Yahya, and O. Mahian, "The Effect of Manifold Zone Parameters on Hydrothermal Performance of micro-channel HeatSink: a Review," *International Journal of Heat and Mass Transfer*, vol. 109, pp. 1143–1161, Jun. 2017, doi: <https://doi.org/10.1016/j.ijheatmasstransfer.2017.03.007>.
- [5] P. B. Jasiński, "Numerical Study of the thermo-hydraulic Characteristics in a Circular Tube with Ball turbulators. Part 1: PIV Experiments and a Pressure Drop," *International Journal of Heat and Mass Transfer/International Journal of Heat and Mass Transfer*, vol. 74, pp. 48–59, Jul. 2014, doi: <https://doi.org/10.1016/j.ijheatmasstransfer.2014.02.074>.
- [6] P. B. Jasiński, "Numerical Study of the thermo-hydraulic Characteristics in a Circular Tube with Ball turbulators. Part 2: Heat Transfer," *International Journal of Heat and Mass Transfer*, vol. 74, pp. 473–483, Jul. 2014, doi: <https://doi.org/10.1016/j.ijheatmasstransfer.2014.02.073>.
- [7] P. B. Jasiński, "Numerical Study of thermo-hydraulic Characteristics in a Circular Tube with Ball turbulators. Part 3: Thermal Performance Analysis," *International Journal of Heat and Mass Transfer*, vol. 107, pp. 1138–1147, Apr. 2017, doi: <https://doi.org/10.1016/j.ijheatmasstransfer.2016.11.017>.
- [8] P. Promthaisong, W. Jedsadaratanachai, and S. Eiamsa-Ard, "Effect of Geometrical Parameters on Turbulent Flow and Heat Transfer Behaviors in triple-start Corrugated Tubes," *Journal of Thermal Science and Technology*, vol. 13, no. 1, pp. JTST0008–JTST0008, Jan. 2018, doi: <https://doi.org/10.1299/jtst.2018jtst0008>.
- [9] C. Man, Xiaogang Lv, T. Hu, P. Sun, and Y. Tang, "Experimental Study on Effect of Heat Transfer Enhancement for single-phase Forced Convective Flow with Twisted Tape Inserts," *International Journal of Heat and Mass Transfer*, vol. 106, pp. 877–883, Mar. 2017, doi: <https://doi.org/10.1016/j.ijheatmasstransfer.2016.10.026>.
- [10] W. Yuan, G. Fang, X. Zhang, Y. Tang, Z. Wan, and S. Zhang, "Heat Transfer and Friction Characteristics of Turbulent Flow through a Circular Tube with Ball Turbulators," *Applied Sciences*, vol. 8, no. 5, p. 776, May 2018, doi: <https://doi.org/10.3390/app8050776>.
- [11] X. Zhang, Z. Liu, and W. Liu, "Numerical Studies on Heat Transfer and Friction Factor Characteristics of a Tube Fitted with Helical screw-tape without core-rod Inserts," *International Journal of Heat and Mass Transfer*, vol. 60, pp. 490–498, May 2013, doi: <https://doi.org/10.1016/j.ijheatmasstransfer.2013.01.041>.
- [12] S. Murthy, R. N. Hegde, and N. Rai, "Conjoint Effect of Turbulator and Al<sub>2</sub>O<sub>3</sub> Nanofluids on DPHEs Thermal performance: Experimental Study," *Heat and Mass Transfer*, vol. 60, no. 6, pp. 933–953, Mar. 2024, doi: <https://doi.org/10.1007/s00231-024-03460-5>.
- [13] A. Veera Kumar, T. V. Arjunan, D. Seenivasan, R. Venkatramanan, S. Vijayan, and M. M. Matheswaran, "Influence of Twisted Tape Inserts on Energy and Exergy Performance of an Evacuated Tube-based Solar Air Collector," *Solar Energy*, vol. 225, pp. 892–904, Sep. 2021, doi: <https://doi.org/10.1016/j.solener.2021.07.074>.
- [14] R. Hosseini, M. Hosseini, and M. Farhadi, "Turbulent Heat Transfer in Tubular Heat Exchangers with Twisted Tape," *Journal of Thermal Analysis and Calorimetry*, vol. 135, no. 3, pp. 1863–1869, Jun. 2018, doi: <https://doi.org/10.1007/s10973-018-7400-y>.
- [15] S. H. Labib *et al.*, "Turbulent Heat Transfer Enhancement in Tubular Heat Exchangers with Different Twisted Tape Inserts," *Journal of Mechanical Engineering And Sciences*, vol. 15, no. 3, pp. 8364–8378, Sep. 2021, doi: <https://doi.org/10.15282/jmes.15.3.2021.14.0658>.
- [16] M. M. K. Bhuiya *et al.*, "Heat Transfer Performance for Turbulent Flow through a Tube Using Double Helical Tape Inserts," *International Communications in Heat and Mass Transfer*, vol. 39, no. 6, pp. 818–825, Jul. 2012, doi: <https://doi.org/10.1016/j.icheatmasstransfer.2012.04.006>.
- [17] J. Luo *et al.*, "Thermal-frictional Behavior of New Special Shape Twisted Tape and Helical Coiled Wire turbulators in Engine Heat Exchangers System," *Case Studies in Thermal Engineering*, vol. 53, pp. 103877–103877, Dec. 2023, doi: <https://doi.org/10.1016/j.csite.2023.103877>.
- [18] S. Eiamsa-ard and P. Promvong, "Thermal Characterization of Turbulent Tube Flows over diamond-shaped Elements in Tandem," *International Journal of Thermal Sciences*, vol. 49, no. 6, pp. 1051–1062, Jun. 2010, doi: <https://doi.org/10.1016/j.ijthermalsci.2009.12.003>.
- [19] G. P. Srivastava, A. K. Patil, and M. Kumar, "Parametric Effect of Diverging Perforated Cones on the thermo-hydraulic Performance of a Heat Exchanger Tube," *Heat and Mass Transfer*, vol. 57, Feb. 2021, doi: <https://doi.org/10.1007/s00231-021-03035-8>.
- [20] M.E. Nakhchi, Javad Abolfazli Esfahani, and K. C. Kim, "Numerical Study of Turbulent Flow inside Heat Exchangers Using Perforated Louvered Strip Inserts," *International Journal of Heat and Mass Transfer*, vol. 148, pp. 119143–119143, Feb. 2020, doi: <https://doi.org/10.1016/j.ijheatmasstransfer.2019.119143>.
- [21] H. Kazemi Moghadam, S. S. Mousavi Ajarostaghi, and S. Poncet, "Extensive Numerical Analysis of the Thermal Performance of a Corrugated Tube with Coiled Wire," *Journal of Thermal Analysis and Calorimetry*, vol. 140, no. 3, pp. 1469–1481, Oct. 2019, doi: <https://doi.org/10.1007/s10973-019-08876-4>.
- [22] B. K. Roomi and M. A. Theeb, "Experimental And Numerical Study Of Inserting An Internal Hollow Core To Finned Helical Coil Tube-Shell Heat Exchanger," *Journal of Engineering and Sustainable Development*, vol. 25, no. 1, pp. 1–14, Feb. 2022, doi: <https://doi.org/10.31272/jeasd.25.1.1>.
- [23] M. Omidi, A. A. Rabienataj Darzi, and M. Farhadi, "Turbulent Heat Transfer and Fluid Flow of Alumina Nanofluid inside three-lobed Twisted Tube," *Journal of Thermal Analysis and Calorimetry*, vol. 137, no. 4, pp. 1451–1462, Jan. 2019, doi: <https://doi.org/10.1007/s10973-019-08026-w>.
- [24] F. R. Menter, "Review of the shear-stress Transport Turbulence Model Experience from an Industrial Perspective," *International Journal of Computational Fluid Dynamics*, vol. 23, no. 4, pp. 305–316, Apr. 2009, doi: <https://doi.org/10.1080/10618560902773387>.
- [25] S. Skullong, P. Promvong, C. Thianpong, and M. Pimsarn, "Heat Transfer and Turbulent Flow Friction in a round Tube with staggered-winglet perforated-tapes," *International Journal of Heat and Mass Transfer*, vol. 95, pp. 230–242, Apr. 2016, doi: <https://doi.org/10.1016/j.ijheatmasstransfer.2015.12.007>.
- [26] H. L. Aneed and D. S. Khudhur, "Numerical Study Of Heat Transfer Enhancement By Inserting Different Size Balls Inside Tube," *Journal of Engineering and Sustainable Development*, vol. 25, no. 6, pp. 1–11, Feb. 2022, doi: <https://doi.org/10.31272/jeasd.25.6.1>.
- [27] R. Karwa, C. Sharma, and N. Karwa, "Performance Evaluation Criterion at Equal Pumping Power for Enhanced Performance Heat Transfer Surfaces," *Journal of Solar Energy*, vol. 2013, pp. 1–9, Jun. 2013, doi: <https://doi.org/10.1155/2013/370823>.
- [28] B. Mohammed and S. Najeeb Shehab, "A Comprehensive Review Study on Heat Transfer Improvement Techniques Within Twisted Tubes," *Journal of Engineering and Sustainable Development*, vol. 27, no. 6, pp. 823–839, Nov. 2023, doi: <https://doi.org/10.31272/jeasd.27.6.12>.